A Unified Impulse Response Model for DCE-MRI

Matthias Christian Schabel[1,2]

[1]*Advanced Imaging Research Center, Oregon Health & Science University, Portland, OR, United States,* [2]*Radiology, University of Utah, Salt Lake City, UT, United States*

Introduction: A number of different impulse response models are in common use for analysis of DCE-MRI data. These include the original Tofts-Kety (TK) and Extended Tofts-Kety (ETK) models as well as the Adiabatic Tissue Homogeneity (ATH) and Two Compartment eXchange (2CX) models. Here we propose a novel generalized approach, termed the Gamma Capillary Transit Time (GCTT) model. This approach mathematically unifies the TK, ETK, ATH, and 2CX models, subsuming them all as limiting cases. By including a model parameter representing the heterogeneity of capillary transit times within a tissue voxel (α^{-1}) in addition to the capillary transit time (t_c), the GCTT model discriminates tissues having relatively monodisperse transit time distributions from those having a large degree of heterogeneity. Each of these five models was fit to DCE-MRI data acquired in three brain tumors (one glioblastoma multiforme, one pleomorphic xanthoastrocytoma, and one anaplastic meningioma) and parameter estimates compared. The ATH, 2CX, and GCTT models all show clear spatial heterogeneity in the distribution of t_c, with the GCTT model giving a broad range of α^{-1} values spanning from the ATH limit ($\alpha^{-1}=0$) to the 2CX limit ($\alpha^{-1}=1$). These *in vivo* results suggest that the GCTT model may be of utility in extracting additional information about tumor physiology from DCE-MRI data beyond what is obtained using current modeling methodologies.

Methods: Beginning from work described in [1], we assume that the distribution of capillary transit times within an imaging voxel can be described by a gamma distribution. The impulse response function (IRF) of the GCTT model can be written in closed form:

$$R^{\mathrm{GCTT}}(t)=\gamma\left(\frac{t_c}{\tau},\frac{t}{\tau}\right)+\frac{Ee^{-k_{ep}t}}{(1-k_{ep}\tau)^{t_c/\tau}}\left[1-\gamma\left(\frac{t_c}{\tau},\left(\frac{1}{\tau}-k_{ep}\right)t\right)\right] \qquad (1)$$

DCE data were acquired on a 3T Siemens scanner under an IRB-approved protocol with a 3D-SPGR sequence. Acquisition parameters were: TR~3ms, TE~1ms, alpha = 20, voxel size~2x2x2 mm, ~3.5 s per frame. Signal data was converted to concentration using the methods described in [2]. The AIF was determined using blind estimation as described in [3]. Nonlinear regression was used to estimate model parameters and Tikhonov-regularized SVD used to determine nonparametric impulse response functions.

Results: The IRF given in Eq. (1) reduces to the TK, ETK, ATH, and 2CX [4] IRFs in various limits, unifying all five models within a conceptual framework. Figure 1 shows measured IRFs (black) for subsets of voxels with low (top) and high (bottom) α^{-1} values. Superimposed are fits of ATH (green), 2CX (red), and GCTT (blue) IRFs. Figure 2 shows maps of GCTT parameters for the GBM.

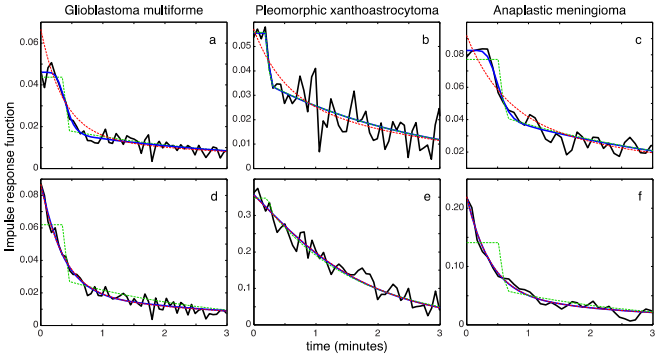

Figure 1. Nonparametric IRFs for voxels with $t_c \geq 15s$ and $\alpha^{-1} \leq 0.25$ (top row) or $\alpha^{-1} \geq 0.75$ (bottom row).

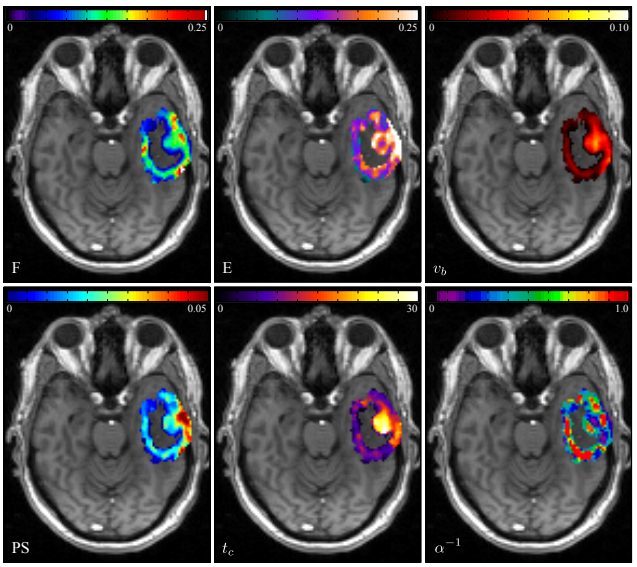

Figure 2. GCTT model parameter maps in a patient with glioblastoma multiforme.

Discussion: Figure 1 demonstrates the existence of tumor regions with tissue IRFs that are similar to the ATH in the $\alpha^{-1}\to 0$ limit (top) and to the 2CX in the $\alpha^{-1}\to 1$ limit (bottom). The GCTT model gives fits that are comparable or superior to the ATH in the former case and that are essentially indistinguishable in the latter. We find that tumor-averaged parameter estimates obtained with the 2CX model generally agreed better with GCTT values than did those obtained with the ATH model. The observation that our model parameter for transit time heterogeneity tended to be large in these brain tumors is consistent with the well-known fact that the tumor microvasculature and blood flow are highly irregular in comparison to normal tissues.

References

1. TS Koh *et al., Phys. Med. Biol.* 2001 **46** 1519-1538.
2. MC Schabel *et al., Phys. Med. Biol.* 2008 **53** 2345-2373.
3. MC Schabel *et al., Phys. Med. Biol.* 2010 **55** 4807-4823.
4. SP Sourbron *et al., Magn. Reson. Med.* 2011 **66** 735-745.